Eur. Phys. J. C (2024) 84:39
https://doi.org/10.1140/epjc/s10052-023-12373-2

THE EUROPEAN PHYSICAL JOURNAL C

Regular Article - Experimental Physics

Determination of the strong-coupling constant from the Z-boson transverse-momentum distribution

Stefano Camarda[1,a], **Giancarlo Ferrera**[2], **Matthias Schott**[3]

[1] CERN, 1211 Geneva, Switzerland
[2] Dipartimento di Fisica, Università di Milano and INFN, Sezione di Milano, 20133 Milan, Italy
[3] Johannes Gutenberg-Universitat Mainz (JGU), Saarstr. 21, 55122 Mainz, Germany

Received: 21 March 2023 / Accepted: 20 December 2023 / Published online: 16 January 2024

Abstract The strong-coupling constant is determined from the low-momentum region of the transverse-momentum distribution of Z bosons produced through the Drell–Yan process, using predictions at third order in perturbative QCD. The analysis employs a measurement performed in proton-antiproton collisions at a centre-of-mass energy of $\sqrt{s} = 1.96$ TeV with the CDF experiment. The determined value of the strong coupling at the reference scale corresponding to the Z-boson mass is $\alpha_S(m_Z) = 0.1191^{+0.0013}_{-0.0016}$.

1 Introduction

The coupling constant of the strong interaction is one of the fundamental parameters of the standard model, and is the least precisely known among the fundamental couplings in nature. The most recent world average of the strong-coupling constant at the scale of the Z-boson mass yields $\alpha_S(m_Z) = 0.1179 \pm 0.0009$, with a relative uncertainty of 0.8% [1]. Various different determinations contribute to the world average, and are categorised according to their methodological approach [2]. The most precise determinations of $\alpha_S(m_Z)$ are from lattice QCD, with a result of $\alpha_S(m_Z) = 0.1184 \pm 0.0008$ [3], and hadronic tau decays, with a result of $\alpha_S(m_Z) = 0.1177 \pm 0.0019$ [1]. Tensions exist between some of the most precise determinations of $\alpha_S(m_Z)$. For instance, several determinations from deep inelastic lepton-nucleon scattering [4–6] and from hadronic final states of electron-positron annihilation [7–9] are significantly lower than the lattice QCD determination. Some of these determinations are performed at next-to-next-to-next-to-leading order (N^{3}LO) in QCD, namely from hadronic tau decays and low Q^2 continuum [10], from non-singlet structure functions in deep inelastic scattering [4], from heavy quarkonia decays [11,12], and from the global fit of the electroweak observables [13,14]. At hadron colliders, the strong-coupling constant has been determined in final states with jets [15,16] from inclusive top quark pairs production [17–19], and more recently from inclusive W and Z bosons production [20]. The high-momentum region of the Z-boson transverse-momentum (p_{T}) distribution measured at the LHC [21–23] was included in parton distribution function (PDF) determinations [24], and contributed to the simultaneous determination of PDFs and strong-coupling constant in Refs. [25–27]. Some of these determinations, in particular those with jets in the final state, allow probing the strong coupling at high values of momentum transfer.

In this context, it is highly desirable to perform alternative determinations of $\alpha_S(m_Z)$ based on new observables and high-order theory predictions, which can help improving the precision in the determination of the strong coupling and resolving existing tensions. This paper presents a new methodology for a precise determination of $\alpha_S(m_Z)$ at hadron colliders from a semi-inclusive (i.e. radiation inhibited) observable, namely the low-momentum Sudakov [28] region of the transverse-momentum distribution of Z bosons produced through the Drell–Yan process [29]. The strong force is responsible for the recoil of the Z bosons, which acquire non-zero transverse momentum from QCD radiation off the initial-state partons, and from non-perturbative intrinsic k_T effects. The hardness of the transverse-momentum distribution is a measure of the strength of the recoil of the Z bosons, which in turn is proportional to the strong coupling. Compared to other determinations of $\alpha_S(m_Z)$ at hadron colliders based on either exclusive or inclusive observables, this determination gathers all desirable features for a precise determination: large observable sensitivity to $\alpha_S(m_Z)$ compared to the experimental precision, high perturbative

[a] e-mail: stefano.camarda@cern.ch (corresponding author)

accuracy of the theoretical prediction [30–34], and in-situ controllable non-perturbative QCD effects [35–45].

The proposed methodology can be applied to proton-antiproton and proton-proton colliders. In this paper we consider proton-antiproton collisions data from the Tevatron collider, because the Drell–Yan process has reduced contribution from heavy-flavour-initiated production, compared to the proton-proton collisions of the LHC. The application to proton-proton collisions can profit from the large high-quality datasets already collected at the LHC experiments, which will be further increased in the future, but could require a more careful study of heavy-flavour-initiated production, and is left to future work.

2 Methodology

The experimental data used in the analysis is the Z-boson transverse-momentum distribution measured with the CDF detector at a centre-of-mass energy of $\sqrt{s} = 1.96$ TeV with 2.1 fb^{-1} of integrated luminosity [46]. The measurement was performed in the electron decay channel, and extrapolated to a kinematic region without requirements on the transverse-momentum and pseudorapidity of the electrons. The extrapolation to full-lepton phase space, which was based on the measured decay lepton angular distributions [47] to avoid significant theoretical uncertainties, enables the usage of fast analytic predictions. In the low-momentum region below 25 GeV, the measurement was performed in bins of Z-boson transverse momentum of 0.5 GeV. The electron resolution for electrons of transverse momentum of 45 GeV was approximately 1 GeV in the central region $|\eta_e| < 1.05$, and 1.5 GeV in the forward region $1.2 < |\eta_e| < 2.8$, enabling small bin-to-bin correlations at the level of 30% for neighbouring bins.

The theoretical predictions are computed with the public numerical program `DYTurbo` [48], which implements the resummation of logarithmically-enhanced contributions in the small-p_{T} region of the leptons pairs at next-to-next-to-next-to-leading-logarithmic (N^{3}LL) accuracy, combined with the hard-collinear contributions at N^{3}LO in powers of the QCD coupling [30]. We briefly review the resummation formalism implemented in `DYTurbo` and developed in Refs. [49–51]. The transverse-momentum resummed cross section for Z-boson[1] production can be written as

$$\mathrm{d}\sigma^{\mathrm{V}} = \mathrm{d}\sigma^{\mathrm{res}} - \mathrm{d}\sigma^{\mathrm{asy}} + \mathrm{d}\sigma^{\mathrm{f.o.}}, \tag{1}$$

where $\mathrm{d}\sigma^{\mathrm{res}}$ is the resummed component of the cross-section, $\mathrm{d}\sigma^{\mathrm{asy}}$ is the asymptotic term that represents the fixed-order expansion of $\mathrm{d}\sigma^{\mathrm{res}}$, and $\mathrm{d}\sigma^{\mathrm{f.o.}}$ is the Z+jet finite-order cross section integrated over final-state QCD radiation. All the cross sections are differential in p_{T}^2. The resummed component $\mathrm{d}\sigma^{\mathrm{res}}$ is the most important term at small p_{T} (i.e. $p_{\mathrm{T}} \ll m_Z$). The finite-order term $\mathrm{d}\sigma^{\mathrm{f.o.}}$ gives the larger net contribution at large p_{T} (i.e. $p_{\mathrm{T}} \sim m_Z$). The fixed-order expansion of the resummed component $\mathrm{d}\sigma^{\mathrm{asy}}$ embodies the singular behaviour of the finite-order term, providing a smooth behaviour of Eq. (1) as p_{T} approaches zero. The resummed component is given by[2]

$$\mathrm{d}\sigma^{\mathrm{res}} = \mathrm{d}\hat{\sigma}^{\mathrm{V}}_{\mathrm{LO}} \times \mathcal{H}_{\mathrm{V}} \times \exp\{\mathcal{G}\} \times S_{\mathrm{NP}}. \tag{2}$$

The term $\mathrm{d}\hat{\sigma}^{\mathrm{V}}_{\mathrm{LO}}$ is the leading-order (LO) cross section.

The function $\mathcal{H}_V$ [52,53] includes the hard-collinear contributions and it can be expanded in powers of α_S as

$$\mathcal{H}_V(\alpha_S) = 1 + \frac{\alpha_S}{\pi}\,\mathcal{H}_V^{(1)} + \left(\frac{\alpha_S}{\pi}\right)^2 \mathcal{H}_V^{(2)} + \left(\frac{\alpha_S}{\pi}\right)^3 \mathcal{H}_V^{(3)} + \cdots . \tag{3}$$

The universal (process independent) form factor $\exp\{\mathcal{G}\}$ contains all the terms that order-by-order in α_S are logarithmically divergent as $p_{\mathrm{T}} \to 0$. The resummed logarithmic expansion of $\mathcal{G}$ reads

$$\begin{aligned}\mathcal{G}(\alpha_S, L) \;&= L\, g^{(1)}(\alpha_S L) + g^{(2)}(\alpha_S L) \\ &\quad + \frac{\alpha_S}{\pi}\, g^{(3)}(\alpha_S L) + \left(\frac{\alpha_S}{\pi}\right)^2 g^{(4)}(\alpha_S L) + \cdots ,\end{aligned} \tag{4}$$

where L is the logarithmic expansion parameter, the functions $g^{(n)}$ control and resum the $\alpha_S^k L^k$ (with $k \geq 1$) logarithmic terms in the exponent of Eq. (2) due to soft and collinear radiation.

The function $\mathcal{G}$ is singular in the region of transverse-momenta of the order of the scale of the QCD coupling Λ_{QCD}. This signals that a truly non-perturbative region is approached and perturbative results are not reliable. The singular behaviour of the perturbative form factor is removed by using the so-called b_* [35,54] regularisation procedure, in which the dependence of $\exp\{\mathcal{G}\}$ on the impact parameter b, that is the Fourier-conjugate variable to p_{T}, is frozen before reaching the singular point by performing the replacement $b^2 \to b_*^2 = b^2 b_{\mathrm{lim}}^2/(b^2 + b_{\mathrm{lim}}^2)$. In the calculation the default value of $b_{\mathrm{lim}} = 3$ GeV^{-1} is used. The minimal prescription [41,55,56] is considered as alternative regularisation procedure.

Concerning non-perturbative corrections of the type Λ^p/M^p, where Λ is the non-perturbative scale of QCD and M is the order of magnitude of the momentum transfer in the process, we note that the dominant power corrections are linear, for instance, in the case of hadronic final states of electron-positron annihilation, whereas they are expected

[1] The contribution from γ^* and its interference with the Z boson are included throughout the calculation.

[2] The convolution with PDFs and the sum over different initial-state partonic contributions are implied in the shorthand notation of Eq. (2).

to be quadratic for the Drell–Yan p_{T} distribution at large p_T [57,58], or, equivalently, in the limit of small b [59]. In the small p_{T} region, the non-perturbative corrections are expected to become linear below some scale [44,60], which is estimated of the order $\mathcal{O}(1\,\mathrm{GeV})$ in Ref. [61]. Determinations of non-perturbative TMD functions from fits to Drell–Yan and semi-inclusive deep inelastic scattering (SIDIS) data further confirm a transition from quadratic to linear behaviour below a scale which is of order $\mathcal{O}(1.5\,\mathrm{GeV})$ for Z-boson production at the Tevatron [62]. The Z-boson p_{T} distribution has negligible sensitivity to non-perturbative corrections below such a small scale. Accordingly, non-perturbative QCD effects are included in this analysis in the form of a Gaussian form factor $S_{\mathrm{NP}} = \exp\{-g\,b^2\}$, which corresponds to a quadratic ansatz for the non-perturbative corrections.

At N^{3}LL+$\mathcal{O}(\alpha_S^3)$ accuracy in the small-p_{T} region (i.e. including all the $\mathcal{O}(\alpha_S^3)$ terms) we have included in the calculation the functions $g^{(4)}$ and $\mathcal{H}_V^{(3)}$ in Eqs. (3) and (4). The asymptotic term $\mathrm{d}\sigma^{\mathrm{asy}}$ and the Z+jet finite-order cross section $\mathrm{d}\sigma^{\mathrm{f.o.}}$ are evaluated at $\mathcal{O}(\alpha_S^3)$. The $\mathcal{O}(\alpha_S^3)$ term of the Z+jet cross section predictions was computed with MCFM [34,63], using a lower cutoff of $p_{\mathrm{T}} = 5$ GeV, and the corresponding $\mathrm{d}\sigma^{\mathrm{f.o.}} - \mathrm{d}\sigma^{\mathrm{asy}}$ matching correction, which is as large as -1% in the Sudakov region, was extrapolated down to $p_{\mathrm{T}} = 0$ by interpolating the corrections with their expected quadratic dependence on p_{T}/m_Z [64], i.e. with the function $(p_{\mathrm{T}}/m_Z)^2 \sum_i c_i \log^i(p_{\mathrm{T}}/m_Z)$ including a set of free parameters c_i (see also Refs. [33,65] for similar parametrisations).

The running of the strong coupling is evaluated at four loops [66,67] consistently in all parts of the calculation. The PDFs are interpolated with LHAPDF [68] at the factorisation scale μ_F, and evolved backward using the next-to-next-to-leading order (NNLO) solution of the evolution equation, as implemented in Ref. [69], and four-loops running of the strong coupling. As shown in Appendix A of Ref. [49], such a procedure consistently resums the N^{3}LL contributions to the form factor. The number of active flavours is set to five in all the coefficients entering the calculation, and in the evolution of the PDFs. In order to assess the impact of charm and bottom thresholds in the PDF evolution, an alternative forward PDF evolution with variable-flavour number scheme is used, and the difference with respect to the nominal five-flavour backward evolution is considered as an uncertainty. The predicted cross sections depend on three unphysical scales: the renormalisation scale μ_R, the factorisation scale μ_F, and the resummation scale Q, which parametrises the arbitrariness in the resummation procedure. The central value of the scales is set to the invariant mass of the lepton pair $m_{\ell\ell}$. We note that within the transverse-momentum resummation formalism of Refs. [49–51] the μ_R, μ_F, and Q scales have to be set of the order of the hard scale of the process $m_{\ell\ell}$ and do not depend on the transverse momentum of the Z boson. The electroweak parameters are set according to the G_μ scheme, in which the Fermi coupling constant G_{F}, the W-boson mass m_W, and the Z-boson mass m_Z are set to the input values $G_{\mathrm{F}} = 1.1663787 \cdot 10^{-5}\,\mathrm{GeV}^{-2}$, $m_W = 80.385$ GeV, $m_Z = 91.1876$ GeV [1], whereas the weak-mixing angle and the QED coupling are calculated at tree level.

The statistical analysis for the determination of $\alpha_S(m_Z)$ is performed with the xFitter framework [70]. The dependence of PDFs on the value of $\alpha_S(m_Z)$ is accounted for by using corresponding α_S-series of PDF sets. The value of $\alpha_S(m_Z)$ is determined by minimising a χ^2 function which includes both the experimental uncertainties and the theoretical uncertainties arising from PDF variations:

$$\begin{aligned}\chi^2(\beta_{\mathrm{exp}}, \beta_{\mathrm{th}}) &= \sum_{i=1}^{N_{\mathrm{data}}} \frac{\left(\sigma_i^{\mathrm{exp}} + \sum_j \Gamma_{ij}^{\mathrm{exp}} \beta_{j,\mathrm{exp}} - \sigma_i^{\mathrm{th}} - \sum_k \Gamma_{ik}^{\mathrm{th}} \beta_{k,\mathrm{th}}\right)^2}{\Delta_i^2} \\ &\quad + \sum_j \beta_{j,\mathrm{exp}}^2 + \sum_k \beta_{k,\mathrm{th}}^2. \end{aligned} \tag{5}$$

The correlated experimental and theoretical uncertainties are included using the nuisance parameter vectors β_{exp} and β_{th}, respectively. Their influence on the data and theory predictions is described by the $\Gamma_{ij}^{\mathrm{exp}}$ and $\Gamma_{ik}^{\mathrm{th}}$ matrices. The index i runs over all N_{data} data points, whereas the index j (k) corresponds to the experimental (theoretical) uncertainty nuisance parameters. The measurements and the uncorrelated experimental uncertainties are given by σ_i^{exp} and Δ_i, respectively, and the theory predictions are σ_i^{th}. At each value of $\alpha_S(m_Z)$, the PDF uncertainties are Hessian profiled according to Eq. (5) [71]. The parameter g of the Gaussian non-perturbative form factor is left free in the fit by adding g variations in Eq. (5) as an unconstrained nuisance parameter. The region of Z-boson transverse momentum $p_{\mathrm{T}} < 30$ GeV is considered in the fit. Initial-state radiation of photons (QED ISR) is estimated at leading-logarithmic accuracy with Pythia8 [72] and the AZ tune of parton shower parameters [21], and the predictions are corrected with a bin-by-bin multiplicative factor. The effect on $\alpha_S(m_Z)$ of including these corrections is $\delta\alpha_S(m_Z) = -0.0006$. Uncertainties are estimated with initial-state photon radiation at next-to-leading logarithmic accuracy [73].

3 Results

The determination of $\alpha_S(m_Z)$ with the Hessian conversion [74] of the NNLO PDF set NNPDF4.0 [75] yields $\alpha_S(m_Z) = 0.1192$, with a statistical uncertainty of ± 0.0007, a systematic experimental uncertainty of ± 0.0001, and a PDF uncertainty of ± 0.0004. The value of g determined in the fit is $g = 0.66 \pm 0.05\,\mathrm{GeV}^2$, with a correlation to $\alpha_S(m_Z)$ of

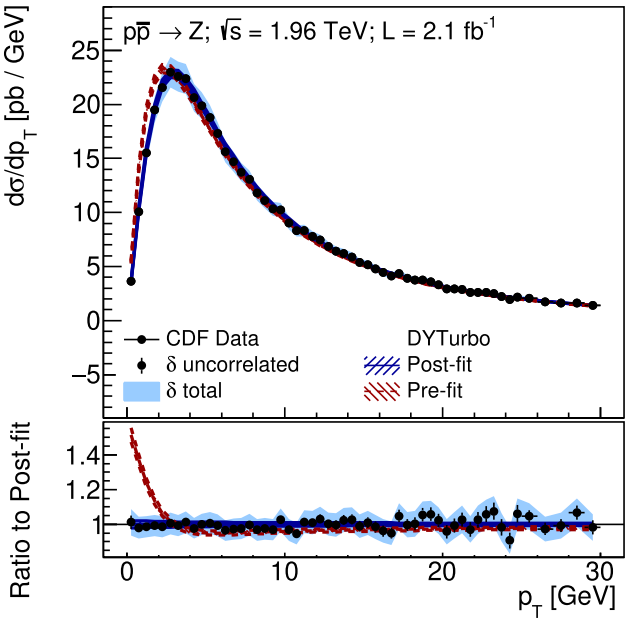

Fig. 1 Comparison of N^{3}LL+$\mathcal{O}(\alpha_S^3)$ DYTurbo predictions to the measured Z-boson transverse-momentum distribution. The settings of the pre- and post-fit predictions are $\alpha_S(m_Z) = 0.118$, $g = 0\,\text{GeV}^2$, and $\alpha_S(m_Z) = 0.1190$, $g = 0.66\,\text{GeV}^2$, respectively. The dashed bands represent the PDF uncertainty of the NNPDF4.0 PDF set

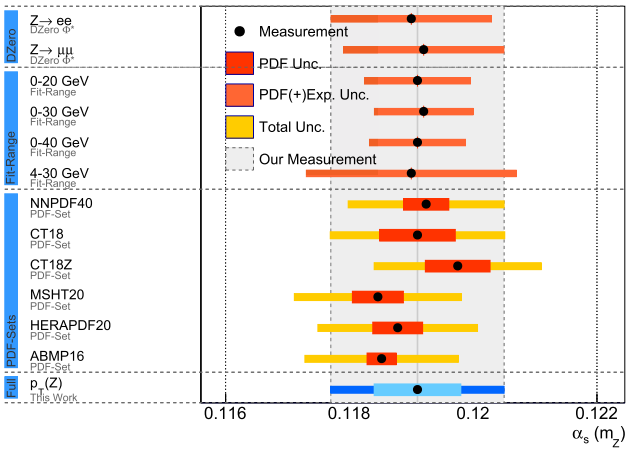

Fig. 2 Comparison of the $\alpha_S(m_Z)$ determination from the Z-boson transverse-momentum distribution with varying fit range, with various different PDF sets, and with measurements performed with the D0 detector

-0.8. When performing a fit with fixed value of g, the uncertainties on $\alpha_S(m_Z)$ are reduced by 30%, yielding an estimate for the uncertainty contribution from non-perturbative QCD effects of ± 0.0006. The value of the χ^2 function at minimum is 41 per 53 degrees of freedom. The pre- and post-fit predictions are compared to the measured Z-boson transverse-momentum distribution in Fig. 1.

Various alternative NNLO PDF sets are considered: CT18 [26], CT18Z, MSHT20 [76], HERAPDF2.0 [77], and ABMP16 [6]. The determined values of $\alpha_S(m_Z)$ range from a minimum of 0.1185 with the MSHT20 PDF set to a maximum of 0.1198 with the CT18Z PDF set. The midpoint value in this range of $\alpha_S(m_Z) = 0.1191$ is considered as nominal result, and the PDF envelope of ± 0.0007 as an additional source of uncertainty. The determination of $\alpha_S(m_Z)$ from the various different NNLO PDF sets is shown in Fig. 2. The approximate N^{3}LO MSHT20 PDF set [78] is also considered, using predictions at approximate next-to-next-to-next-to-next-to-leading-logarithmic (N^{4}LL) accuracy [79], yielding a value of $\alpha_S(m_Z) = 0.1184$. Determinations of $\alpha_S(m_Z)$ at hadron colliders are exposed to possible biases unless the PDFs are determined simultaneously along with $\alpha_S(m_Z)$ [80]. Nonetheless, $\alpha_S(m_Z)$ determinations from single or limited hadron collider datasets based on existing PDF sets, are interesting to study in detail the sensitivity to $\alpha_S(m_Z)$ of a particular observable and the associated theoretical uncertainties. The Hessian profiling employed in this analysis provides an approximation to a PDF determination which relies on the accuracy of the quadratic approximation around the minimum [81] (see Appendix B for details). In all the cases considered in this analysis, pulls and constraints of the nuisance parameters associated to the PDF uncertainties are below 20% and 10%, respectively, indicating that the new minimum of the profiled PDFs is very close to the original minimum, which gives confidence in the validity of the quadratic approximation.

With the aim of further testing the validity of the Hessian profiling approximation, a simultaneous fit of PDFs, $\alpha_S(m_Z)$, and the non-perturbative parameter g is performed. The combined neutral and charged current deep inelastic scattering (DIS) cross-section data from the H1 and ZEUS experiments at the HERA collider [77] are included in the fit, with a minimum squared four-momentum transfer Q^2 of 3.5 GeV^2, together with the Z-boson transverse-momentum distribution measured by CDF. The light-quark coefficient functions of the DIS cross sections are calculated in the $\overline{MS}$ scheme [82], and with the renormalisation and factorisation scales set to the squared four-momentum transfer Q^2. The heavy quarks c and b are dynamically generated, and the corresponding coefficient functions for the neutral-current processes with γ^* exchange are calculated in the general-mass variable-flavour-number (VFN) scheme [83–85], with up to five active quark flavours. The charm mass is set to $m_c = 1.43$ GeV, and the bottom mass to $m_b = 4.50$ GeV [77]. For the charged-current processes the heavy quarks are treated as massless. The PDFs for the gluon, u-valence, d-valence, $\bar{u}$, $\bar{d}$ quark densities are parameterised at the input scale $Q_0^2 = 1.9\,\text{GeV}^2$ with the parametrisation of Ref. [77]. The contribution of the s-quark density is taken to be proportional to the $\bar{d}$-quark density by setting $x\bar{s}(x) = r_s x\bar{d}(x)$, with $r_s = 0.67$. The determined value of $\alpha_S(m_Z)$ from this fit is 0.1184 ± 0.0006, where the quoted uncertainty is the

uncertainty from the fit, which includes experimental and PDF uncertainties. The value of $\alpha_S(m_Z)$ is in agreement with the determinations based on the Hessian profiling approach.

The alternative fits with different PDF sets and the simultaneous fit of PDFs and $\alpha_S(m_Z)$ are summarised in Table 1.

Missing higher order uncertainties are estimated through independent variations of μ_R, μ_F and Q in the range $m_{\ell\ell}/2 \leq \{\mu_R, \mu_F, Q\} \leq 2m_{\ell\ell}$ with the constraints $0.5 \leq \{\mu_F/\mu_R, Q/\mu_R, Q/\mu_F\} \leq 2$, leading to 14 variations. The determined values of $\alpha_S(m_Z)$ range from a minimum of 0.1183 to a maximum of 0.1196 with respect to the value at the central scale choice of $\alpha_S(m_Z) = 0.1192$, yielding a scale-variation envelope of $^{+0.0004}_{-0.0009}$. The alternative fits with different choices of the QCD scales are summarised in Table 2.

Fits without the $\mathcal{O}(\alpha_S^3)$ matching corrections yield a central value which is 0.0005 lower, and an increase in the half envelope of scale variations from 0.0007 to 0.0009, which is consistent with the observed shift. Systematic uncertainties in the $\mathcal{O}(\alpha_S^3)$ matching corrections are estimated by raising the lower cutoff from $p_{\mathrm{T}} = 5$ GeV to $p_{\mathrm{T}} = 10$ GeV. The difference of 0.0001 with respect to the nominal fit is considered as a source of uncertainty. Statistical uncertainties in the $\mathcal{O}(\alpha_S^3)$ matching corrections are estimated with a set of 1000 replicas of the matching corrections generated by fluctuating them within their numerical uncertainties. The upper and lower limits of the 68% confidence level envelope of interpolations to the replicas are used for the estimate of the statistical uncertainty, yielding less than ± 0.0001. Further details are provided in Appendix A.

Uncertainties in the modelling of the non-perturbative form factor are estimated by performing four alternative fits with: a value of $b_{\mathrm{lim}} = 2\ \mathrm{GeV}^{-1}$ in the b_* regularisation procedure; the minimal prescription, which corresponds to the limit $b_{\mathrm{lim}} \to \infty$; using an additional quartic term $\exp\{-q\, b^4\}$ with $q = 0.1\ \mathrm{GeV}^4$; using the additional term $\exp\{-g_k\}$ with $g_k = g_0\big(1 - \exp\big[-\frac{C_F}{\pi g_0 b_{\mathrm{lim}}^2}\big]\big)\log(m_{\ell\ell}^2/Q_0^2)$ with $g_0 = 0.3$, $Q_0 = 1$ GeV, and $b_{\mathrm{lim}} = 2\ \mathrm{GeV}^{-1}$ [44], where C_F is the colour-factor associated with gluon emission from a quark. The alternative fits yield variations of $\alpha_S(m_Z)$ in the range of ± 0.0007, which is considered as an uncertainty. In the alternative fits, the parameter of the Gaussian non-perturbative form factor ranges from $g = 0.42\ \mathrm{GeV}^2$ in the case of the minimal prescription to $g = 0.83\ \mathrm{GeV}^2$ in the case of the fit with $b_{\mathrm{lim}} = 2\ \mathrm{GeV}^{-1}$, in agreement with values obtained by global fits [42,86,87], and corresponding to values of average primordial k_T^2 of the partons, $\langle k_T^2 \rangle = 2\, g$ [88,89], in the range 0.8–1.7 GeV^2. Such values are generally large for non-perturbative effects within a bound state with a mass of 1 GeV as the proton. However the fitted values of g also accounts for power corrections related to the regularisation procedure of the perturbative form factor, to the perturbative evolution of the non-perturbative form factor from low scales to m_Z, and to yet uncalculated higher-order corrections. A fit in which the NNPDF4.0 PDF set is evolved with a variable-flavour number scheme yields $\delta\alpha_S(m_Z) = -0.0003$, which is considered as an additional source of uncertainty. The alternative fits with different non-perturbative and heavy flavour models are summarised in Table 3.

A fit with NLL initial-state radiation of photons yields a difference on $\alpha_S(m_Z)$with respect to the PYTHIA8 modelling of less than 0.0001, which is considered as an additional source of uncertainty.

The stability of the results upon variations of the fit range is tested by performing fits in the regions of Z-boson transverse momentum $p_{\mathrm{T}} < 20$ GeV and $p_{\mathrm{T}} < 40$ GeV. The spread in the determined values of $\alpha_S(m_Z)$ is at the level of ± 0.0001 and the uncertainty of the fit increases from ± 0.0007 to ± 0.0008. Since the region $20 < p_{\mathrm{T}} < 40$ GeV is sensitive to the matching of the resummed cross section to the fixed order prediction, this test provides a confirmation that the result is largely independent from the matching corrections in this region. Uncertainties associated to the stability of the fit results with respect to variations of the upper limit of the fit range are considered negligible. The fit range is also varied by excluding the low transverse-momentum region. The range is reduced up to $4 < p_{\mathrm{T}} < 30$ GeV, with a spread in the values of $\alpha_S(m_Z)$ at the level of ± 0.0002, and an increase in the uncertainty of the fit from ± 0.0008 to ± 0.0016. For the fit in the range $4 < p_{\mathrm{T}} < 30$ GeV the value of g is determined as $0.3 \pm 0.3\ \mathrm{GeV}^2$ and the correlation between $\alpha_S(m_Z)$ and g is reduced from -0.8 to -0.4. Since the low transverse-momentum region is the most sensitive to the non-perturbative QCD effects, this test provides a validation of the model for the non-perturbative form factor. The spread of ± 0.0002 from variations of the lower limit of the fit range is considered as an additional source of uncertainty.

A consistency check of the $\alpha_S(m_Z)$ determination was performed using cross sections measured with the D0 detector [90]. The fit to the D0 data in the Z-boson rapidity range $|y| < 1$ yields value of $\alpha_S(m_Z) = 0.1190 \pm 0.0013$ in the electron decay channel and $\alpha_S(m_Z) = 0.1192 \pm 0.0013$ in the muon decay channel, where the quoted uncertainties include experimental and PDF uncertainties. The D0 measurement, which was performed on the variable ϕ_η^*, is extrapolated to the transverse-momentum p_{T}. The extrapolation procedure has associated uncertainties which were not estimated in the analysis. The determined values of $\alpha_S(m_Z)$ are compatible with the CDF result within experimental uncertainties. Determinations of $\alpha_S(m_Z)$ with varying fit range and with cross sections measured with the D0 detector are shown in Fig. 2.

A summary of the uncertainties in the determination of $\alpha_S(m_Z)$ is shown in Table 4.

Table 1 Alternative fits of $\alpha_S(m_Z)$ with different PDF sets

	$\alpha_S(m_Z)$	g [GeV^2]	χ^2/dof
NNPDF4.0	0.1192 ± 0.0008	0.66 ± 0.05	41/53
CT18	0.1189 ± 0.0010	0.67 ± 0.05	40/53
CT18Z	0.1198 ± 0.0009	0.62 ± 0.05	41/53
MSHT20	0.1185 ± 0.0009	0.72 ± 0.05	40/53
HERAPDF2.0	0.1188 ± 0.0008	0.69 ± 0.05	40/53
ABMP16	0.1185 ± 0.0007	0.62 ± 0.05	42/53
MSHT20an3lo (N^{4}LL)	0.1184 ± 0.0009	0.73 ± 0.05	40/53
PDF fit	0.1184 ± 0.0006	0.71 ± 0.05	1405/1184

Table 2 Alternative fits of $\alpha_S(m_Z)$ with different choices of the renormalisation (μ_R), factorisation (μ_F) and resummation (Q) scales

$\mu_R/m_{\ell\ell}$	$\mu_F/m_{\ell\ell}$	$Q/m_{\ell\ell}$	$\alpha_S(m_Z)$	g [GeV^2]	χ^2/dof
1	1	1	0.1192 ± 0.0008	0.66 ± 0.05	41/53
1	1	2	0.1183 ± 0.0007	0.77 ± 0.05	40/53
1	1	0.5	0.1196 ± 0.0008	0.57 ± 0.05	42/53
1	2	1	0.1194 ± 0.0008	0.66 ± 0.05	41/53
1	2	2	0.1183 ± 0.0007	0.77 ± 0.05	41/53
1	0.5	1	0.1193 ± 0.0008	0.68 ± 0.05	42/53
1	0.5	0.5	0.1196 ± 0.0008	0.59 ± 0.05	42/53
2	1	1	0.1193 ± 0.0008	0.67 ± 0.05	42/53
2	1	2	0.1194 ± 0.0008	0.70 ± 0.05	41/53
2	2	1	0.1192 ± 0.0008	0.65 ± 0.05	42/53
2	2	2	0.1192 ± 0.0008	0.67 ± 0.05	41/53
0.5	1	1	0.1184 ± 0.0007	0.75 ± 0.05	42/53
0.5	1	0.5	0.1192 ± 0.0007	0.64 ± 0.05	41/53
0.5	0.5	1	0.1183 ± 0.0007	0.75 ± 0.05	42/53
0.5	0.5	0.5	0.1192 ± 0.0007	0.64 ± 0.05	42/53

Table 3 Alternative fits of $\alpha_S(m_Z)$ with different non-perturbative and heavy flavour models

	$\alpha_S(m_Z)$	g [GeV^2]	χ^2/dof
$b_{\lim} = 2$ GeV^{-1}	0.1187 ± 0.0007	0.83 ± 0.05	43/53
$b_{\lim} \to \infty$	0.1199 ± 0.0008	0.42 ± 0.05	41/53
g_k	0.1186 ± 0.0008	0.65 ± 0.05	46/53
$q = 0.1$ GeV^4	0.1197 ± 0.0008	0.51 ± 0.05	41/53
VFN PDF evolution	0.1190 ± 0.0007	0.71 ± 0.05	59/53

Table 4 Summary of the uncertainties for the determination of $\alpha_S(m_Z)$, in units of 10^{-3}

Statistical uncertainty	± 0.7	
Experimental systematic uncertainty	± 0.1	
PDF uncertainty (NNPDF4.0)	± 0.4	
PDF uncertainty (envelope of PDFs)	± 0.7	
Scale variations uncertainties	+0.4	− 0.9
Matching at $\mathcal{O}(\alpha_S^3)$	± 0.1	
Non-perturbative model	± 0.7	
Flavour model	0	− 0.3
QED ISR	$< \pm 0.1$	
Lower limit of fit range	± 0.2	
Total	+1.3	− 1.6

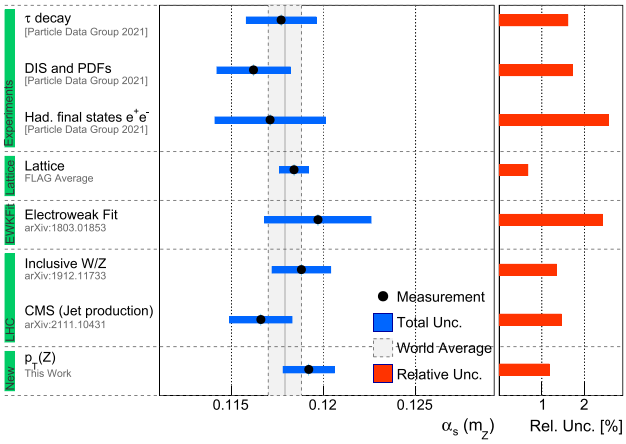

Fig. 3 Comparison of the $\alpha_S(m_Z)$ determination from the Z-boson transverse-momentum distribution to other determinations and to the world-average value

4 Conclusions

In summary, the value of the strong-coupling constant determined in this analysis is $\alpha_S(m_Z) = 0.1191^{+0.0013}_{-0.0016}$, with a statistical uncertainty of ± 0.0007, an experimental systematic uncertainty of ± 0.0001, a PDF uncertainty of ± 0.0008, missing higher order uncertainties of $^{+0.0004}_{-0.0009}$, and additional theory uncertainties (non-perturbative model, flavour scheme, matching corrections, photon initial-state radiation) of ± 0.0008. The strong-coupling constant is also determined in a simultaneous PDF-fit determination including DIS cross-section data from the H1 and ZEUS experiments at the HERA collider. When considering the fit uncertainties of ± 0.0006 and all the other relevant uncertainties listed in Table 4, the result of this determination is $\alpha_S(m_Z) = 0.1184^{+0.0013}_{-0.0015}$.

We have performed a determination of $\alpha_S(m_Z)$ from the Z-boson transverse-momentum distribution measured at the Tevatron collider, in the low-momentum region of $p_{\mathrm{T}} < 30$ GeV. This analysis represents the first determination using QCD resummed theory predictions based on a semi-inclusive observable at hadron-hadron colliders.[3] The PDF uncertainties are estimated with a conservative approach, including the envelope of six different PDF sets, and with a Hessian profiling procedure, which avoids possible biases in the treatment of PDF uncertainties. Missing higher order uncertainties are estimated with the standard approach of computing an envelope of scale variations. The measured value of $\alpha_S(m_Z)$ has a relative uncertainty of 1.2%, and is compatible with other determinations and with the world-average value, as illustrated in Fig. 3.

Among hadron colliders determination, this is the most precise to date and the first based on N^{3}LL+$\mathcal{O}(\alpha_S^3)$ predictions in perturbative QCD.

[3] Analogous QCD resummed theory predictions in electron-positron collisions were used to determine $\alpha_S(m_Z)$ at LEP [7–9,91–93].

Acknowledgements We gratefully acknowledge Willis Sakumoto for providing the correlation matrix of the CDF Z-boson transverse-momentum measurement, Tobias Neumann for providing the MCFM NNLO Z+jet predictions, Pier Monni for suggesting to include variations of the lower edge of the fit range, Dave Soper for fruitful discussions, and Sasha Glazov and Stefano Catani for useful comments on the manuscript. This research used resources of the National Energy Research Scientific Computing Center (NERSC), a U.S. Department of Energy Office of Science User Facility located at Lawrence Berkeley National Laboratory, operated under Contract No. DE-AC02-05CH11231 using NERSC award HEP-ERCAP0021890.

Data Availability Statement This manuscript has no associated data or the data will not be deposited. [Authors' comment: This is a phenomenological study based on a previously published measurement by the CDF Collaboration. All theory predictions can be calculated using existing public codes.].

Funded by SCOAP[3].

A Matching corrections

In this Appendix we discuss the interpolation of the $\mathrm{d}\sigma^{\mathrm{f.o.}} - \mathrm{d}\sigma^{\mathrm{asy}}$ matching corrections of Eq. (1) at $\mathcal{O}(\alpha_S^3)$ with their expected quadratic dependence on p_{T}/m_Z using the function

$$\frac{p_{\mathrm{T}}^2}{m_Z^2} \sum_i c_i \ln^i \left(\frac{p_{\mathrm{T}}}{m_Z} \right). \tag{6}$$

Fits are performed in the region of $p_{\mathrm{T}} < 50$ GeV, with 10 logarithmically spaced bins. The p-values for fits of the matching corrections with different choices of the renormalisation, factorisation, and resummation scales are in the range from 0.3 to 0.9.

We have considered two sources of uncertainties addressing the statistical and systematic uncertainties of the matching corrections. We have varied the lower cutoff from $p_T = 5$ GeV to $p_T = 10$ GeV. The difference in $\alpha_S(m_Z)$ of 0.0001 is considered as an additional systematic uncertainty. In order to estimate the statistical uncertainty, we have generated a set of 1000 Monte Carlo replicas of the matching corrections, by fluctuating them within their numerical uncertainties. The upper and lower limits of the 68% confidence level envelope of the extrapolation fits to the 1000 replicas are used for the estimate of the statistical uncertainty, yielding ± 0.00002 on $\alpha_S(m_Z)$.

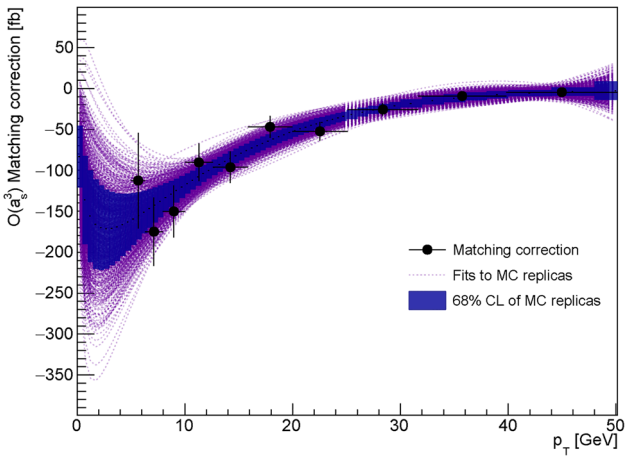

Fig. 4 The $\mathcal{O}(\alpha_S^3)$ matching corrections

The difference between the NNLO Z+jet predictions and the expansion of the resummed calculation, showing the numerical accuracy in the matching procedure at α_S^3 order, is presented in Fig. 4, which also shows the replicas and their 68% confidence level uncertainty band.

Comparable figures showing the difference of the asymptotic term $\mathrm{d}\sigma^{\mathrm{asy}}$ and the Z+jet finite-order cross section $\mathrm{d}\sigma^{\mathrm{f.o.}}$ at $\mathcal{O}(\alpha_S^3)$ can be found in Refs. [30,33,34,64]

The studies of statistical and systematic uncertainties discussed above confirm that the $\mathcal{O}(\alpha_S^3)$ matching corrections are associated with small uncertainties, which are accounted for in the final result. The estimated uncertainties of ± 0.0001 are consistent with the overall small impact of such corrections, which is estimated as $+0.0005$.

B Simultaneous PDF and $\alpha_S(m_Z)$ fit

The Hessian profiling employed in this analysis provides an approximation to a PDF determination which relies on the accuracy of the quadratic approximation around the minimum [81]. The validity of the Hessian profiling approximation, is verified by performing a simultaneous fit of PDFs, $\alpha_S(m_Z)$, and the the parameter g of the Gaussian non-perturbative form factor, with a setup similar to the one employed for the HERAPDF2.0 [77] PDF determination. In this Appendix we provide further quantitative details of the comparison of the Hessian profiling of HERAPDF2.0 with such a PDF fit. The PDF fit includes the combined neutral and charged current deep inelastic scattering (DIS) cross-section data from the H1 and ZEUS experiments at the HERA collider [77]. Table 5 shows the contribution to the total χ^2 of the various datasets used in the fit, compared to the χ^2 of the Hessian profiling, and a comparison of the determined values of $\alpha_S(m_Z)$ and g.

Table 5 Comparison of the Hessian profiling of HERAPDF2.0 with the PDF fit, including the contribution to the total χ^2 at minimum of the various datasets used in the fit

	PDF fit	Hessian profiling
$\alpha_S(m_Z)$	0.1188 ± 0.0008	0.1184 ± 0.0006
g [GeV^2]	0.69 ± 0.05	0.71 ± 0.05
Dataset	χ^2/points	χ^2/points
NC DIS H1-ZEUS e^+p	955/905	
CC DIS H1-ZEUS e^+p	46/39	
NC DIS H1-ZEUS e^-p	219/159	
CC DIS H1-ZEUS e^-p	53/42	
H1-ZEUS correlated χ^2	91	
CDF Z p_{T}	41/55	40/55
Total	1405 / 1184	

References

1. Particle Data Group Collaboration, P. A. Zyla et al., Review of Particle Physics. *PTEP* **8**, 083C01 (2020). https://doi.org/10.1093/ptep/ptaa104
2. G. P. Salam, *The strong coupling: a theoretical perspective*, pp. 101–121 (2019). https://doi.org/10.1142/9789813238053_0007. arXiv:1712.0516 [hep-ph]
3. Flavour Lattice Averaging Group (FLAG) Collaboration, Y. Aoki et al., FLAG Review 2021. Eur. Phys. J. C **82**(10), 869 (2022). https://doi.org/10.1140/epjc/s10052-022-10536-1. arXiv:2111.09849 [hep-lat]
4. J. Blumlein, H. Bottcher, A. Guffanti, Non-singlet QCD analysis of deep inelastic world data at O(alpha(s)**3). Nucl. Phys. B **774**, 182–207 (2007). https://doi.org/10.1016/j.nuclphysb.2007.03.035. arXiv:hep-ph/0607200
5. P. Jimenez-Delgado, E. Reya, Delineating parton distributions and the strong coupling. Phys. Rev. D **89**(7), 074049 (2014). https://doi.org/10.1103/PhysRevD.89.074049. arXiv:1403.1852 [hep-ph]
6. S. Alekhin, J. Blümlein, S. Moch, R. Placakyte, Parton distribution functions, α_s, and heavy-quark masses for LHC Run II. Phys. Rev. D **96**(1), 014011 (2017). https://doi.org/10.1103/PhysRevD.96.014011. arXiv:1701.05838 [hep-ph]
7. R. Abbate, M. Fickinger, A.H. Hoang, V. Mateu, I.W. Stewart, Thrust at N^3LL with Power Corrections and a Precision Global Fit for $\alpha_s(mZ)$. Phys. Rev. D **83**, 074021 (2011). https://doi.org/10.1103/PhysRevD.83.074021. arXiv:1006.3080 [hep-ph]
8. T. Gehrmann, G. Luisoni, P.F. Monni, Power corrections in the dispersive model for a determination of the strong coupling constant from the thrust distribution. Eur. Phys. J. C **73**(1), 2265 (2013). https://doi.org/10.1140/epjc/s10052-012-2265-x. arXiv:1210.6945 [hep-ph]
9. A.H. Hoang, D.W. Kolodrubetz, V. Mateu, I.W. Stewart, Precise determination of α_s from the C-parameter distribution. Phys. Rev. D **91**(9), 094018 (2015). https://doi.org/10.1103/PhysRevD.91.094018. arXiv:1501.04111 [hep-ph]
10. P.A. Baikov, K.G. Chetyrkin, J.H. Kuhn, Order alpha**4(s) QCD Corrections to Z and tau Decays. Phys. Rev. Lett. **101**, 012002 (2008). https://doi.org/10.1103/PhysRevLett.101.012002. arXiv:0801.1821 [hep-ph]
11. V. Mateu, P.G. Ortega, Bottom and Charm Mass determinations from global fits to $Q\bar{Q}$ bound states at N^{3}LO. JHEP **01**, 122 (2018). https://doi.org/10.1007/JHEP01(2018)122. arXiv:1711.05755 [hep-ph]

12. C. Peset, A. Pineda, J. Segovia, The charm/bottom quark mass from heavy quarkonium at N^{3}LO. JHEP **09**, 167 (2018). https://doi.org/10.1007/JHEP09(2018)167. arXiv:1806.05197 [hep-ph]
13. J. Haller, A. Hoecker, R. Kogler, K. Mönig, T. Peiffer, J. Stelzer, Update of the global electroweak fit and constraints on two-Higgs-doublet models. Eur. Phys. J. C **78**(8), 675 (2018). https://doi.org/10.1140/epjc/s10052-018-6131-3. arXiv:1803.01853 [hep-ph]
14. D. d'Enterria, V. Jacobsen, Improved strong coupling determinations from hadronic decays of electroweak bosons at N^{3}LO accuracy. arXiv:2005.04545 [hep-ph]
15. C.M.S. Collaboration, A. Tumasyan et al., Measurement and QCD analysis of double-differential inclusive jet cross sections in proton-proton collisions at $\sqrt{s}$ = 13 TeV. JHEP **02**, 142 (2022). https://doi.org/10.1007/JHEP02(2022)142. arXiv:2111.10431 [hep-ex]. [Addendum: JHEP 12, 035 (2022)]
16. ATLAS Collaboration, M. Aaboud et al., Determination of the strong coupling constant α_s from transverse energy–energy correlations in multijet events at $\sqrt{s} = 8$ TeV using the ATLAS detector. Eur. Phys. J. C **77**(12), 872 (2017). https://doi.org/10.1140/epjc/s10052-017-5442-0. arXiv:1707.02562 [hep-ex]
17. C.M.S. Collaboration, A.M. Sirunyan et al., Measurement of the $t\bar{t}$ production cross section, the top quark mass, and the strong coupling constant using dilepton events in pp collisions at $\sqrt{s} =$ 13 TeV. Eur. Phys. J. C **79**(5), 368 (2019). https://doi.org/10.1140/epjc/s10052-019-6863-8. arXiv:1812.10505 [hep-ex]
18. CMS Collaboration, S. Chatrchyan et al., Determination of the Top-Quark Pole Mass and Strong Coupling Constant from the $t\bar{t}$ Production Cross Section in pp Collisions at $\sqrt{s} = 7$ TeV. Phys. Lett. B **728**, 496–517 (2014). https://doi.org/10.1016/j.physletb.2013.12.009. arXiv:1307.1907 [hep-ex]. [Erratum: Phys.Lett.B 738, 526–528 (2014)]
19. T. Klijnsma, S. Bethke, G. Dissertori, G.P. Salam, Determination of the strong coupling constant $\alpha_s(m_Z)$ from measurements of the total cross section for top-antitop quark production. Eur. Phys. J. C **77**(11), 778 (2017). https://doi.org/10.1140/epjc/s10052-017-5340-5. arXiv:1708.07495 [hep-ph]
20. D. d'Enterria, A. Poldaru, Extraction of the strong coupling $\alpha_s(\mathrm{m}_Z)$ from a combined NNLO analysis of inclusive electroweak boson cross sections at hadron colliders. JHEP **06**, 016 (2020). https://doi.org/10.1007/JHEP06(2020)016. arXiv:1912.11733 [hep-ph]
21. ATLAS Collaboration, G. Aad et al., Measurement of the Z/γ^* boson transverse momentum distribution in pp collisions at $\sqrt{s} =$ 7 TeV with the ATLAS detector. JHEP **09**, 145 (2014). https://doi.org/10.1007/JHEP09(2014)145. arXiv:1406.3660 [hep-ex]
22. ATLAS Collaboration, G. Aad et al., Measurement of the transverse momentum and ϕ^*_η distributions of Drell–Yan lepton pairs in proton–proton collisions at $\sqrt{s} = 8$ TeV with the ATLAS detector. Eur. Phys. J. C **76**(5), 291 (2016). https://doi.org/10.1140/epjc/s10052-016-4070-4. arXiv:1512.02192 [hep-ex]
23. C.M.S. Collaboration, V. Khachatryan et al., Measurement of the Z boson differential cross section in transverse momentum and rapidity in proton–proton collisions at 8 TeV. Phys. Lett. B **749**, 187–209 (2015). https://doi.org/10.1016/j.physletb.2015.07.065. arXiv:1504.03511 [hep-ex]
24. R. Boughezal, A. Guffanti, F. Petriello, M. Ubiali, The impact of the LHC Z-boson transverse momentum data on PDF determinations. JHEP **07**, 130 (2017). https://doi.org/10.1007/JHEP07(2017)130. arXiv:1705.00343 [hep-ph]
25. NNPDF Collaboration, R. D. Ball, S. Carrazza, L. Del Debbio, S. Forte, Z. Kassabov, J. Rojo, E. Slade, M. Ubiali, Precision determination of the strong coupling constant within a global PDF analysis. Eur. Phys. J. C **78**(5), 408 (2018). https://doi.org/10.1140/epjc/s10052-018-5897-7. arXiv:1802.03398 [hep-ph]
26. T.-J. Hou et al., New CTEQ global analysis of quantum chromodynamics with high-precision data from the LHC. Phys. Rev. D **103**(1), 014013 (2021). https://doi.org/10.1103/PhysRevD.103.014013. arXiv:1912.10053 [hep-ph]
27. T. Cridge, L.A. Harland-Lang, A.D. Martin, R.S. Thorne, An investigation of the α_S and heavy quark mass dependence in the MSHT20 global PDF analysis. Eur. Phys. J. C **81**(8), 744 (2021). https://doi.org/10.1140/epjc/s10052-021-09533-7. arXiv:2106.10289 [hep-ph]
28. V.V. Sudakov, Vertex parts at very high-energies in quantum electrodynamics. Sov. Phys. JETP **3**, 65–71 (1956)
29. S. D. Drell, T.-M. Yan, Massive lepton-pair production in hadron-hadron collisions at high energies. Phys. Rev. Lett. **25**, 902–902 (1970). https://doi.org/10.1103/PhysRevLett.25.902.2
30. S. Camarda, L. Cieri, G. Ferrera, Drell–Yan lepton-pair production: qT resummation at N3LL accuracy and fiducial cross sections at N3LO. Phys. Rev. D **104**(11), L111503 (2021). https://doi.org/10.1103/PhysRevD.104.L111503. arXiv:2103.04974 [hep-ph]
31. E. Re, L. Rottoli, P. Torrielli, Fiducial Higgs and Drell-Yan distributions at N^{3}LL′+NNLO with RadISH. arXiv:2104.07509 [hep-ph]
32. W.-L. Ju, M. Schönherr, The q_T and $\Delta\phi$ spectra in W and Z production at the LHC at N^{3}LL'+N^{2}LO. JHEP **10**, 088 (2021). https://doi.org/10.1007/JHEP10(2021)088. arXiv:2106.11260 [hep-ph]
33. X. Chen, T. Gehrmann, E.W.N. Glover, A. Huss, P.F. Monni, E. Re, L. Rottoli, P. Torrielli, Third-Order Fiducial Predictions for Drell-Yan Production at the LHC. Phys. Rev. Lett. **128**(25), 252001 (2022). https://doi.org/10.1103/PhysRevLett.128.252001. arXiv:2203.01565 [hep-ph]
34. T. Neumann, J. Campbell, Fiducial Drell-Yan production at the LHC improved by transverse-momentum resummation at N4LLp+N3LO. Phys. Rev. D **107**(1), L011506 (2023). https://doi.org/10.1103/PhysRevD.107.L011506. arXiv:2207.07056 [hep-ph]
35. J.C. Collins, D.E. Soper, G.F. Sterman, Transverse Momentum Distribution in Drell-Yan Pair and W and Z Boson Production. Nucl. Phys. B **250**, 199–224 (1985). https://doi.org/10.1016/0550-3213(85)90479-1
36. C. T. H. Davies, B. R. Webber, W. J. Stirling, Drell-Yan Cross-Sections at Small Transverse Momentum
37. G.A. Ladinsky, C.P. Yuan, The Nonperturbative regime in QCD resummation for gauge boson production at hadron colliders. Phys. Rev. D **50**, R4239 (1994). https://doi.org/10.1103/PhysRevD.50.R4239. arXiv:hep-ph/9311341
38. R.K. Ellis, D.A. Ross, S. Veseli, Vector boson production in hadronic collisions. Nucl. Phys. B **503**, 309–338 (1997). https://doi.org/10.1016/S0550-3213(97)00403-3. arXiv:hep-ph/9704239
39. F. Landry, R. Brock, G. Ladinsky, C.P. Yuan, New fits for the nonperturbative parameters in the CSS resummation formalism. Phys. Rev. D **63**, 013004 (2000). https://doi.org/10.1103/PhysRevD.63.013004. arXiv:hep-ph/9905391
40. J.-W. Qiu, X.-F. Zhang, Role of the nonperturbative input in QCD resummed Drell-Yan Q_T distributions. Phys. Rev. D **63**, 114011 (2001). https://doi.org/10.1103/PhysRevD.63.114011. arXiv:hep-ph/0012348
41. A. Kulesza, G.F. Sterman, W. Vogelsang, Joint resummation in electroweak boson production. Phys. Rev. D **66**, 014011 (2002). https://doi.org/10.1103/PhysRevD.66.014011. arXiv:hep-ph/0202251
42. A.V. Konychev, P.M. Nadolsky, Universality of the Collins-Soper-Sterman nonperturbative function in gauge boson production. Phys. Lett. B **633**, 710–714 (2006). https://doi.org/10.1016/j.physletb.2005.12.063. arXiv:hep-ph/0506225
43. M. Guzzi, P.M. Nadolsky, B. Wang, Nonperturbative contributions to a resummed leptonic angular distribution in inclusive neutral vector boson production. Phys. Rev. D **90**(1), 014030 (2014). https://doi.org/10.1103/PhysRevD.90.014030. arXiv:1309.1393 [hep-ph]
44. J. Collins, T. Rogers, Understanding the large-distance behavior of transverse-momentum-dependent parton densities and the Collins-

Soper evolution kernel. Phys. Rev. D **91**(7), 074020 (2015). https://doi.org/10.1103/PhysRevD.91.074020. arXiv:1412.3820 [hep-ph]
45. S.-Y. Wei, Exploring the non-perturbative Sudakov factor via Z^0 -boson production in pp collisions. Phys. Lett. B **817**, 136356 (2021). https://doi.org/10.1016/j.physletb.2021.136356. arXiv:2009.06514 [hep-ph]
46. CDF Collaboration, T. Aaltonen et al., Transverse momentum cross section of e^+e^- pairs in the Z-boson region from $p\bar{p}$ collisions at $\sqrt{s} = 1.96$ TeV. Phys. Rev. D **86**, 052010 (2012). https://doi.org/10.1103/PhysRevD.86.052010. arXiv:1207.7138 [hep-ex]
47. CDF Collaboration, T. Aaltonen et al., First Measurement of the Angular Coefficients of Drell-Yan e^+e^- pairs in the Z Mass Region from $p\bar{p}$ Collisions at $\sqrt{s}$ = 1.96 TeV. Phys. Rev. Lett. **106**, 241801 (2011). https://doi.org/10.1103/PhysRevLett.106.241801. arXiv:1103.5699 [hep-ex]
48. S. Camarda et al., DYTurbo: Fast predictions for Drell-Yan processes. Eur. Phys. J. C **80**(3), 251 (2020). https://doi.org/10.1140/epjc/s10052-020-7757-5. arXiv:1910.07049 [hep-ph]. [Erratum: Eur.Phys.J.C 80, 440 (2020)]
49. G. Bozzi, S. Catani, D. de Florian, M. Grazzini, Transverse-momentum resummation and the spectrum of the Higgs boson at the LHC. Nucl. Phys. B **737**, 73–120 (2006). https://doi.org/10.1016/j.nuclphysb.2005.12.022. arXiv:hep-ph/0508068
50. G. Bozzi, S. Catani, G. Ferrera, D. de Florian, M. Grazzini, Production of Drell-Yan lepton pairs in hadron collisions: Transverse-momentum resummation at next-to-next-to-leading logarithmic accuracy. Phys. Lett. B **696**, 207–213 (2011). https://doi.org/10.1016/j.physletb.2010.12.024. arXiv:1007.2351 [hep-ph]
51. S. Catani, D. de Florian, G. Ferrera, M. Grazzini, Vector boson production at hadron colliders: transverse-momentum resummation and leptonic decay. JHEP **12**, 047 (2015). https://doi.org/10.1007/JHEP12(2015)047. arXiv:1507.06937 [hep-ph]
52. S. Catani, D. de Florian, M. Grazzini, Universality of nonleading logarithmic contributions in transverse momentum distributions. Nucl. Phys. B **596**, 299–312 (2001). https://doi.org/10.1016/S0550-3213(00)00617-9. arXiv:hep-ph/0008184
53. S. Catani, L. Cieri, D. de Florian, G. Ferrera, M. Grazzini, Universality of transverse-momentum resummation and hard factors at the NNLO. Nucl. Phys. B **881**, 414–443 (2014). https://doi.org/10.1016/j.nuclphysb.2014.02.011. arXiv:1311.1654 [hep-ph]
54. J.C. Collins, D.E. Soper, Back-To-Back Jets: Fourier Transform from B to K-Transverse. Nucl. Phys. B **197**, 446–476 (1982). https://doi.org/10.1016/0550-3213(82)90453-9
55. S. Catani, M.L. Mangano, P. Nason, L. Trentadue, The Resummation of soft gluons in hadronic collisions. Nucl. Phys. B **478**, 273–310 (1996). https://doi.org/10.1016/0550-3213(96)00399-9. arXiv:hep-ph/9604351
56. E. Laenen, G.F. Sterman, W. Vogelsang, Higher order QCD corrections in prompt photon production. Phys. Rev. Lett. **84**, 4296–4299 (2000). https://doi.org/10.1103/PhysRevLett.84.4296. arXiv:hep-ph/0002078
57. S. Ferrario Ravasio, G. Limatola, P. Nason, Infrared renormalons in kinematic distributions for hadron collider processes. JHEP **06**, 018 (2021). https://doi.org/10.1007/JHEP06(2021)018. arXiv:2011.14114 [hep-ph]
58. F. Caola, S. Ferrario Ravasio, G. Limatola, K. Melnikov, P. Nason, On linear power corrections in certain collider observables. JHEP **01**, 093 (2022). https://doi.org/10.1007/JHEP01(2022)093. arXiv:2108.08897 [hep-ph]
59. S. Tafat, Nonperturbative corrections to the Drell–Yan transverse momentum distribution. JHEP **05**, 004 (2001). https://doi.org/10.1088/1126-6708/2001/05/004. arXiv:hep-ph/0102237
60. A.A. Vladimirov, Self-contained definition of the Collins–Soper kernel. Phys. Rev. Lett. **125**(19), 192002 (2020). https://doi.org/10.1103/PhysRevLett.125.192002. arXiv:2003.02288 [hep-ph]
61. P. Schweitzer, M. Strikman, C. Weiss, Intrinsic transverse momentum and parton correlations from dynamical chiral symmetry breaking. JHEP **01**, 163 (2013). https://doi.org/10.1007/JHEP01(2013)163. arXiv:1210.1267 [hep-ph]
62. I. Scimemi, A. Vladimirov, Non-perturbative structure of semi-inclusive deep-inelastic and Drell-Yan scattering at small transverse momentum. JHEP **06**, 137 (2020). https://doi.org/10.1007/JHEP06(2020)137. arXiv:1912.06532 [hep-ph]
63. R. Boughezal, J.M. Campbell, R.K. Ellis, C. Focke, W.T. Giele, X. Liu, F. Petriello, Z-boson production in association with a jet at next-to-next-to-leading order in perturbative QCD. Phys. Rev. Lett. **116**(15), 152001 (2016). https://doi.org/10.1103/PhysRevLett.116.152001. arXiv:1512.01291 [hep-ph]
64. S. Camarda, L. Cieri, G. Ferrera, Fiducial perturbative power corrections within the $\mathbf{q}_T$ subtraction formalism. Eur. Phys. J. C **82**(6), 575 (2022). https://doi.org/10.1140/epjc/s10052-022-10510-x. arXiv:2111.14509 [hep-ph]
65. G. Billis, B. Dehnadi, M.A. Ebert, J.K.L. Michel, F.J. Tackmann, Higgs pT spectrum and total cross section with fiducial cuts at third resummed and fixed order in QCD. Phys. Rev. Lett. **127**(7), 072001 (2021). https://doi.org/10.1103/PhysRevLett.127.072001. arXiv:2102.08039 [hep-ph]
66. T. van Ritbergen, J.A.M. Vermaseren, S.A. Larin, The Four loop beta function in quantum chromodynamics. Phys. Lett. B **400**, 379–384 (1997). https://doi.org/10.1016/S0370-2693(97)00370-5. arXiv:hep-ph/9701390
67. M. Czakon, The Four-loop QCD beta-function and anomalous dimensions. Nucl. Phys. B **710**, 485–498 (2005). https://doi.org/10.1016/j.nuclphysb.2005.01.012. arXiv:hep-ph/0411261
68. A. Buckley, J. Ferrando, S. Lloyd, K. Nordström, B. Page, M. Rüfenacht, M. Schönherr, G. Watt, LHAPDF6: parton density access in the LHC precision era. Eur. Phys. J. C **75**, 132 (2015). https://doi.org/10.1140/epjc/s10052-015-3318-8. arXiv:1412.7420 [hep-ph]
69. A. Vogt, Efficient evolution of unpolarized and polarized parton distributions with QCD-PEGASUS. Comput. Phys. Commun. **170**, 65–92 (2005). https://doi.org/10.1016/j.cpc.2005.03.103. arXiv:hep-ph/0408244
70. S. Alekhin et al., HERAFitter. Eur. Phys. J. C **75**(7), 304 (2015). https://doi.org/10.1140/epjc/s10052-015-3480-z. arXiv:1410.4412 [hep-ph]
71. HERAFitter developers' Team Collaboration, S. Camarda et al., QCD analysis of W- and Z-boson production at Tevatron. Eur. Phys. J. C 75(9), 458 (2015). https://doi.org/10.1140/epjc/s10052-015-3655-7. arXiv:1503.05221 [hep-ph]
72. T. Sjöstrand, S. Ask, J.R. Christiansen, R. Corke, N. Desai, P. Ilten, S. Mrenna, S. Prestel, C.O. Rasmussen, P.Z. Skands, An introduction to PYTHIA 8.2. Comput. Phys. Commun. **191**, 159–177 (2015). https://doi.org/10.1016/j.cpc.2015.01.024. arXiv:1410.3012 [hep-ph]
73. L. Cieri, G. Ferrera, G.F.R. Sborlini, Combining QED and QCD transverse-momentum resummation for Z boson production at hadron colliders. JHEP **08**, 165 (2018). https://doi.org/10.1007/JHEP08(2018)165. arXiv:1805.11948 [hep-ph]
74. S. Carrazza, S. Forte, Z. Kassabov, J.I. Latorre, J. Rojo, An unbiased hessian representation for Monte Carlo PDFs. Eur. Phys. J. C **75**(8), 369 (2015). https://doi.org/10.1140/epjc/s10052-015-3590-7. arXiv:1505.06736 [hep-ph]
75. NNPDF Collaboration, R. D. Ball et al., The path to proton structure at 1% accuracy. Eur. Phys. J. C **82**(5), 428 (2022). https://doi.org/10.1140/epjc/s10052-022-10328-7. arXiv:2109.02653 [hep-ph]
76. S. Bailey, T. Cridge, L.A. Harland-Lang, A.D. Martin, R.S. Thorne, Parton distributions from LHC, HERA, Tevatron and fixed target data: MSHT20 PDFs. Eur. Phys. J. C **81**(4), 341 (2021). https://doi.org/10.1140/epjc/s10052-021-09057-0. arXiv:2012.04684 [hep-ph]

77. H1, ZEUS Collaboration, H. Abramowicz et al., Combination of measurements of inclusive deep inelastic $e^{\pm}p$ scattering cross sections and QCD analysis of HERA data. Eur. Phys. J. C **75**(12), 580 (2015). https://doi.org/10.1140/epjc/s10052-015-3710-4. arXiv:1506.06042 [hep-ex]
78. J. McGowan, T. Cridge, L. A. Harland-Lang, R. S. Thorne, Approximate N^{3}LO parton distribution functions with theoretical uncertainties: MSHT20aN^{3}LO PDFs. Eur. Phys. J. C **83**(3), 185 (2023). https://doi.org/10.1140/epjc/s10052-023-11236-0. arXiv:2207.04739 [hep-ph]. [Erratum: Eur.Phys.J.C 83, 302 (2023)]
79. S. Camarda, L. Cieri, G. Ferrera, Drell–Yan lepton-pair production: q_T resummation at approximate N^{4}LL+N^{4}LO accuracy. arXiv:2303.12781 [hep-ph]
80. S. Forte, Z. Kassabov, Why α_s cannot be determined from hadronic processes without simultaneously determining the parton distributions. Eur. Phys. J. C **80**(3), 182 (2020). https://doi.org/10.1140/epjc/s10052-020-7748-6. arXiv:2001.04986 [hep-ph]
81. H. Paukkunen, P. Zurita, PDF reweighting in the Hessian matrix approach. JHEP **12**, 100 (2014). https://doi.org/10.1007/JHEP12(2014)100. arXiv:1402.6623 [hep-ph]
82. S. Weinberg, New approach to the renormalization group. Phys. Rev. D **8**, 3497–3509 (1973). https://doi.org/10.1103/PhysRevD.8.3497
83. R.S. Thorne, R.G. Roberts, Ordered analysis of heavy flavor production in deep-inelastic scattering. Phys. Rev. D **57**, 6871–6898 (1998). https://doi.org/10.1103/PhysRevD.57.6871. arXiv:hep-ph/9709442
84. R.S. Thorne, Variable-flavor number scheme for next-to-next-to-leading order. Phys. Rev. D **73**, 054019 (2006). https://doi.org/10.1103/PhysRevD.73.054019. arXiv:hep-ph/0601245
85. R.S. Thorne, Effect of changes of variable flavor number scheme on parton distribution functions and predicted cross sections. Phys. Rev. D **86**, 074017 (2012). https://doi.org/10.1103/PhysRevD.86.074017. arXiv:1201.6180 [hep-ph]
86. A. Bacchetta, V. Bertone, C. Bissolotti, G. Bozzi, F. Delcarro, F. Piacenza, M. Radici, Transverse-momentum-dependent parton distributions up to N^{3}LL from Drell-Yan data. JHEP **07**, 117 (2020). https://doi.org/10.1007/JHEP07(2020)117. arXiv:1912.07550 [hep-ph]
87. P. Sun, J. Isaacson, C.P. Yuan, F. Yuan, Nonperturbative functions for SIDIS and Drell-Yan processes. Int. J. Mod. Phys. A **33**(11), 1841006 (2018). https://doi.org/10.1142/S0217751X18410063. arXiv:1406.3073 [hep-ph]
88. G. Parisi, R. Petronzio, Small Transverse Momentum Distributions in Hard Processes. Nucl. Phys. B **154**, 427–440 (1979). https://doi.org/10.1016/0550-3213(79)90040-3
89. M. Hirai, H. Kawamura, K. Tanaka, New determination of the nonperturbative form factor in QCD transverse-momentum resummation for vector boson production. In *20th International Workshop on Deep-Inelastic Scattering and Related Subjects*, pp. 535–538 (2012). https://doi.org/10.3204/DESY-PROC-2012-02/136
90. D0 Collaboration, V. M. Abazov et al., Precise Study of the Z/γ^* Boson Transverse Momentum Distribution in $p\bar{p}$ Collisions using a Novel Technique. Phys. Rev. Lett. 106, 122001 (2011). https://doi.org/10.1103/PhysRevLett.106.122001. arXiv:1010.0262 [hep-ex]
91. S. Bethke, S. Catani, A summary of alpha-s measurements. In *27th Rencontres de Moriond: QCD and High-energy Hadronic Interactions*, pp. 203–208 (1992)
92. S. Catani, L. Trentadue, G. Turnock, B.R. Webber, Resummation of large logarithms in e+ e- event shape distributions. Nucl. Phys. B **407**, 3–42 (1993). https://doi.org/10.1016/0550-3213(93)90271-P
93. A. Verbytskyi, A. Banfi, A. Kardos, P.F. Monni, S. Kluth, G. Somogyi, Z. Szőr, Z. Trócsányi, Z. Tulipánt, G. Zanderighi, High precision determination of α_s from a global fit of jet rates. JHEP **08**, 129 (2019). https://doi.org/10.1007/JHEP08(2019)129. arXiv:1902.08158 [hep-ph]